β-Catenin Defines Head Versus Tail Identity During Planarian Regeneration and Homeostasis

Kyle A. Gurley, *et al.*

Science **319**, 323 (2008);
DOI: 10.1126/science.1150029

its highest ($17.5 million) when up to 2 km^2 of mangroves are allowed to be converted to shrimp aquaculture and the remainder of the ecosystem is preserved. This outcome also yields a more equitable distribution across stakeholders (Fig. 2B), which may be an important objective in any EBM strategy for coastal management. Local mangrove-dependent coastal communities and other coastal communities living within 5 km inland would obtain approximately the same share of economic benefits from the mangrove system ($15.6 and $13.2 million, respectively), but now outside investors would earn some commercial profits from shrimp farming ($1.9 million). Finally, we note that the outcome from our Thailand mangrove valuation example corresponds to "best practice" guidelines for mangrove management in Asia, which recommend that ideal mangrove/pond ratios should not exceed 20% of the habitat area converted to ponds (*23*, *24*).

By including nonlinear relationships in an economic valuation of ecosystem services, our results challenge the assumption that the competing demands of coastal interface systems must always result in either conservation or habitat destruction. As the case study of Thailand mangroves illustrates, the way in which ecological and economic analysis is combined to estimate the values of various ecosystem services can have a large impact on coastal EBM outcome. If point estimates of these values are used to project linear relationships between the benefits of ecosystem services with respect to changes in key ecosystem physical attributes, such as area or distance from shore, then the result might be to force EBM decision-making into a simple "all or none" choice. This result is at odds with EBM strategies, which emphasize reconciliation between economic development pressures and conservation of critical ecosystem resources and services (*5*–*8*). However, if the nonlinear ecological function underlying a service, such as coastal protection afforded by mangroves, is incorporated into economic valuation, then we more realistically represent how ecosystem services change with habitat conversion and how EBM may best be used.

References and Notes

1. Coastal areas are defined in (*2*, *3*) as habitat from the low water mark (<50 m depth) to the coastline and inland from the coastline to a maximum of 100 km or 50-m elevation (whichever is closer to the sea).
2. *Marine and Coastal Ecosystems and Human Well-Being: A Synthesis Report Based on the Findings of the Millennium Ecosystem Assessment* (UN Environment Programme, Nairobi, 2006).
3. Millennium Ecosystem Assessment, *Ecosystems and Human Well-Being: Current State and Trends* (Island, Washington, DC, 2005), chap. 19.
4. I. Valiela, J. Bowen, J. York, *Bioscience* **51**, 807 (2001).
5. K. McLeod, J. Lubchenco, S. Palumbi, A. Rosenberg, Scientific Consensus Statement on Marine Ecosystem-Based Management (Communication Partnership for Science and the Sea, 2005; http://compassonline.org/marinescience/solutions_ecosystem.asp).
6. T.-E. Chua, D. Bonga, N. Bermas-Atrigenio, *Coast. Manage.* **34**, 303 (2006).
7. *Ecosystem-Based Management: Markers for Assessing Progress* (UN Environment Programme/GPA, The Hague, 2006).
8. P. Kareiva, S. Watts, R. McDonald, T. Boucher, *Science* **316**, 1866 (2007).
9. A. Balmford *et al*., *Science* **297**, 950 (2002).
10. L. Brander, R. Florax, J. Vermaat, *Environ. Resour. Econ.* **33**, 223 (2006).
11. E. Barbier, *Econ. Policy* **22**, 177 (2007).
12. K. Gaston, T. Blackborn, *Pattern and Process in Macroecology* (Blackwell Science, Oxford, ed. 2, 2000).
13. J. Petersen *et al*., *Bioscience* **53**, 1181 (2003).
14. E. Farnsworth, *Global Ecol. Biogeogr. Lett.* **7**, 15 (1998).
15. See supporting material on *Science* Online.
16. E. Barbier, *Contemp. Econ. Policy* **21**, 59 (2003).
17. S. Sathirathai, E. Barbier, *Contemp. Econ. Policy* **19**, 109 (2001).
18. S. Massel, K. Furukawa, R. Brinkman, *Fluid Dyn. Res.* **24**, 219 (1999).
19. Y. Mazda, M. Magi, M. Kogo, P. N. Hong, *Mangroves Salt Marshes* **1**, 127 (1997).
20. Y. Mazda, M. Magi, Y. Ikeda, T. Kurokawa, T. Asano, *Wetlands Ecol. Manage.* **14**, 365 (2006).
21. E. Wolanski, in *Coastal Protection in the Aftermath of the Indian Ocean Tsunami: What Role for Forests and Trees?*, S. Braatz, S. Fortuna, J. Broadhead, R. Leslie, Eds. (FAO, Bangkok, 2007), pp. 157–179.
22. The wave attenuation relationship of fig. S1A was transformed into percent wave reduction as a function of 100-m inland mangrove distance, and this relationship was used to adjust the net present value per km^2 estimate for storm protection used in Fig. 1A, assuming that each km^2 of mangroves deforested involved the equivalent loss of 100 m of mangroves inland along the 10-km coastline. See (*15*) for details.
23. P. Saenger, E. Hegerl, J. Davie, *Global Status of Mangrove Ecosystems* (IUCN, Gland, Switzerland, 1983).
24. J. Primavera *et al*., *Bull. Mar. Sci.* **80**, 795 (2007).

25. This work was conducted as part of the "Measuring ecological, economic, and social values of coastal habitats to inform ecosystem-based management of land-sea interfaces" Working Group supported by the National Center for Ecological Analysis and Synthesis, funded by NSF grant DEB-0553768; the University of California, Santa Barbara; the State of California; and the David and Lucile Packard Foundation. We thank B. Halpern for his assistance with this project and work, and three anonymous reviewers for their constructive comments.

Supporting Online Material

www.sciencemag.org/cgi/content/full/319/5861/321/DC1
Materials and Methods
Figs. S1 and S2
Tables S1 to S3
References

11 September 2007; accepted 22 November 2007
10.1126/science.1150349

β-Catenin Defines Head Versus Tail Identity During Planarian Regeneration and Homeostasis

Kyle A. Gurley, Jochen C. Rink, Alejandro Sánchez Alvarado*

After amputation, freshwater planarians properly regenerate a head or tail from the resulting anterior or posterior wound. The mechanisms that differentiate anterior from posterior and direct the replacement of the appropriate missing body parts are unknown. We found that in the planarian *Schmidtea mediterranea*, RNA interference (RNAi) of β-*catenin* or *dishevelled* causes the inappropriate regeneration of a head instead of a tail at posterior amputations. Conversely, RNAi of the β-catenin antagonist *adenomatous polyposis coli* results in the regeneration of a tail at anterior wounds. In addition, the silencing of β-*catenin* is sufficient to transform the tail of uncut adult animals into a head. We suggest that β-catenin functions as a molecular switch to specify and maintain anteroposterior identity during regeneration and homeostasis in planarians.

β-Catenin is a multifunctional protein that controls transcriptional output as well as cell adhesion. During embryonic development of both vertebrates and invertebrates, β-catenin regulates a variety of cellular processes, including organizer formation, cell fate specification, proliferation, and differentiation (*1*–*9*). In adult animals, the Wnt/β-catenin pathway participates in regeneration and tissue homeostasis; misregulation of this pathway can lead to degenerative diseases and cancer in humans (*9*–*12*). In response to upstream cues, such as Wnt ligands binding to Frizzled receptors, β-catenin accumulates in nuclei (Fig. 1A) and invokes transcriptional responses that direct the specification and patterning of tissues (*13*, *14*). Adenomatous polyposis coli (APC) is an essential member of a destruction complex that phosphorylates β-catenin, resulting in its constitutive degradation. Hence, loss of APC leads to a rise in β-catenin levels that is sufficient to drive transcriptional responses (*15*). The intracellular protein Dishevelled has multiple functions but plays an essential role as a positive regulator of β-catenin by inhibiting the destruction complex (*16*).

As part of a systematic effort to define the roles of signaling pathways in planaria, we analyzed the canonical Wnt signaling system in *Schmidtea mediterranea*. We cloned and determined the expression patterns of all identifiable homologs of core pathway components (Fig. 1A) and silenced them, individually or in combina-

Department of Neurobiology and Anatomy, Howard Hughes Medical Institute, University of Utah School of Medicine, 401 MREB, 20N 1900E, Salt Lake City, UT 84132, USA.

*To whom correspondence should be addressed. E-mail: sanchez@neuro.utah.edu

tions, on the basis of likelihood of redundancy as gleaned from the expression data (figs. S1 to S6 and table S1). RNAi-treated animals were then amputated to assess the role of the silenced genes during regeneration (Fig. 1B). After head and tail amputations of control worms, the remaining trunk formed one anterior and one posterior blastema, which then differentiated to replace the missing structures (Fig. 1C; $n = 28$). However, RNAi of a single β-*catenin* (*Smed-*β*catenin-1*), both *dishevelled* homologs (*Smed-dvl-1;Smed-dvl-2*), or *APC* (*Smed-APC-1*) caused striking alterations in the anteroposterior (A/P) identity of regenerating tissues (Fig. 1, D to F). Both blastemas of *Smed-*β*catenin-1(RNAi)* worms adopted an anterior fate, resulting in animals with two heads of opposite orientation (penetrance = 100%, $n = 39$). *Smed-dvl-1(RNAi);Smed-dvl-2(RNAi)* worms also regenerated heads from both blastemas but displayed additional phenotypes, including ectopic and supernumerary photoreceptors in the anterior region. This is consistent with the multiple roles of Dishevelled in different pathways (Fig. 1E; penetrance = 75%, $n = 20$). On the other hand, *Smed-APC-1(RNAi)* animals regenerated tails from both amputation planes (Fig. 1F; penetrance = 60%, $n = 43$).

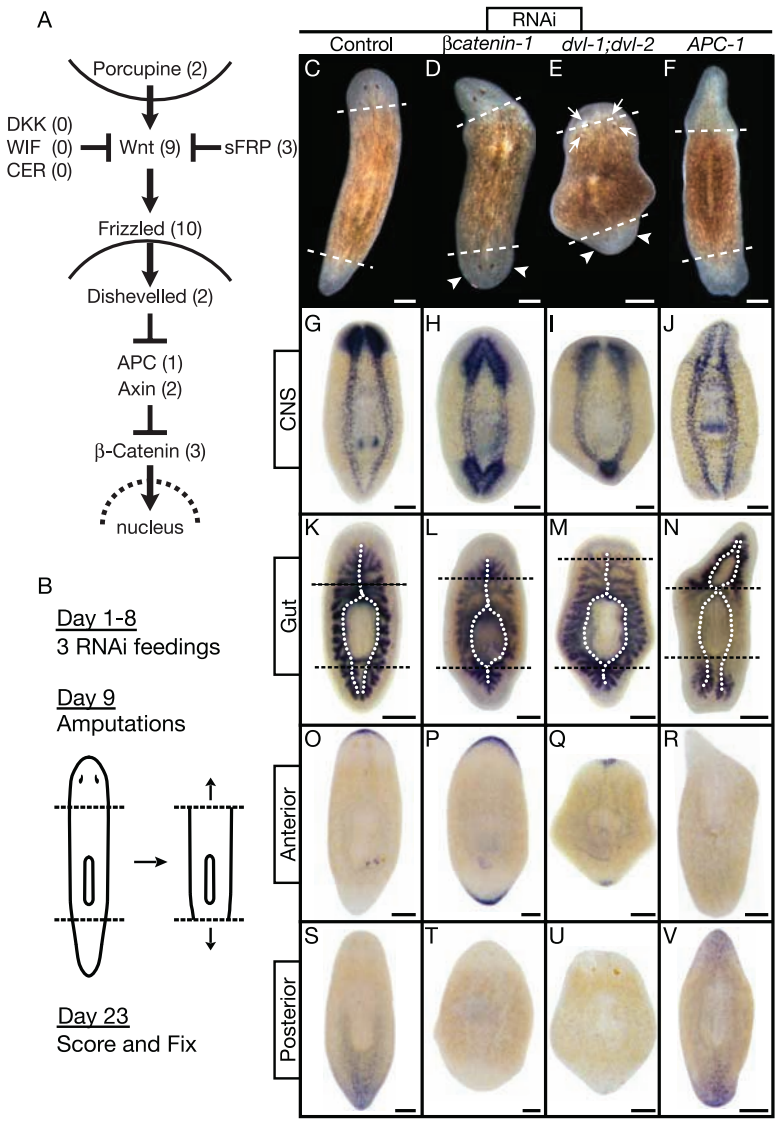

Fig. 1. Signaling through β-catenin defines head versus tail during regeneration. (**A**) Canonical Wnt pathway. Numbers denote *S. mediterranea* homologs identified and silenced. (**B**) Experimental strategy. (**C** to **V**) Trunk fragments 14 days after amputation. Dashed lines, amputation planes; control, *unc-22(RNAi)*. (C) to (F): Live animals. (D) and (E): *Smed-*β*catenin-1(RNAi)* and *Smed-dvl-1(RNAi);Smed-dvl-2(RNAi)* posterior blastemas formed heads with photoreceptors (arrowheads). *Smed-dvl-1(RNAi);Smed-dvl-2(RNAi)* fragments also developed ectopic photoreceptors, often within old tissues (arrows). (F): *Smed-APC-1(RNAi)* anterior blastemas formed tails. (G) to (V): In situ hybridizations ($n \geq 5$ per marker). Markers: CNS, prohormone convertase 2 (PC2); gut, *porcupine* (*Smed-porcn-1*); anterior, *secreted frizzled-related protein* (*Smed-sFRP-1*); posterior, *frizzled* (*Smed-fz-4*). (G) and (K): Normal brain and ventral nerve cords; single anterior and dual posterior gut branches (dotted lines). (H), (I), (L), and (M): *Smed-*β*catenin-1(RNAi)* and *Smed-dvl-1(RNAi);Smed-dvl-2(RNAi)* posterior blastemas developed brain tissue and head-like gut branches. (J) and (N): *Smed-APC-1(RNAi)* anterior blastemas developed tail-like nerve cords and gut branches. (O) and (S): Normal anterior and posterior marker expression. (P), (Q), (T), and (U): *Smed-*β*catenin-1(RNAi)* and *Smed-dvl-1(RNAi);Smed-dvl-2(RNAi)* induced anterior marker expression at both ends, whereas the posterior marker was virtually undetectable. (R) and (V): *Smed-APC-1(RNAi)* induced posterior marker expression at both ends, whereas the anterior marker was virtually undetectable. Scale bars, 200 μm.

To address whether these changes were superficial or reflected a fate transformation of internal cell types and organ systems, we used anatomical and molecular markers of A/P identity. Anatomically, two organ systems with characteristic asymmetries along the A/P axis were examined: (i) the central nervous system (CNS), composed of two anterior cephalic ganglia (brain) and two ventral cords projecting posteriorly (Fig. 1G), and (ii) the digestive system, consisting of a single anterior and two posterior gut branches (Fig. 1K). The "posterior" head of *Smed-*β*catenin-1(RNAi)* and *Smed-dvl-1(RNAi);Smed-dvl-2(RNAi)* animals contained a characteristically anterior nervous system and gut, as did the "anterior" head (Fig. 1, H, I, L, and M). In contrast, the "anterior" tail of *Smed-APC-1(RNAi)* animals was devoid of discernible brain tissue and exhibited posterior structures, as did the "posterior" tail (Fig. 1, J and N).

To define the molecular extent of A/P misspecification, we used two markers identified during our in situ analyses that are specifically expressed at the anterior and posterior ends of intact and regenerating animals (Fig. 1, A, O, and S). *Smed-sFRP-1,* a homolog of secreted Frizzled-related proteins (sFRP), was expressed in an arch of cells capping the anterior edge of the animal. In contrast, *Smed-fz-4*, a homolog of Frizzled receptors, was expressed at the posterior edge in a posterior-to-anterior gradient. We refer to *Smed-sFRP-1* and *Smed-fz-4* as the "anterior marker" and the "posterior marker," respectively, in all subsequent analyses.

In *Smed-*β*catenin-1(RNAi)* and *Smed-dvl-1(RNAi);Smed-dvl-2(RNAi)* worms, the "posterior" head expressed the anterior marker, whereas the posterior marker was severely reduced or absent (Fig. 1, P, Q, T, and U). Conversely, the "anterior" tail of *Smed-APC-1(RNAi)* animals expressed the posterior marker, whereas the anterior marker was severely reduced or absent (Fig. 1, R and V). We noted that misspecified heads and tails in RNAi-treated worms moved independently from the rest of the animal, hence this tissue was functioning autonomously (movies S1 to S3). We conclude that silencing *Smed-*β*catenin-1*, *Smed-dvl-1(RNAi);Smed-dvl-2(RNAi)*, or *Smed-APC-1* is sufficient to misspecify blastema identity.

The inappropriate regeneration of complete heads and tails in RNAi-treated animals sug-

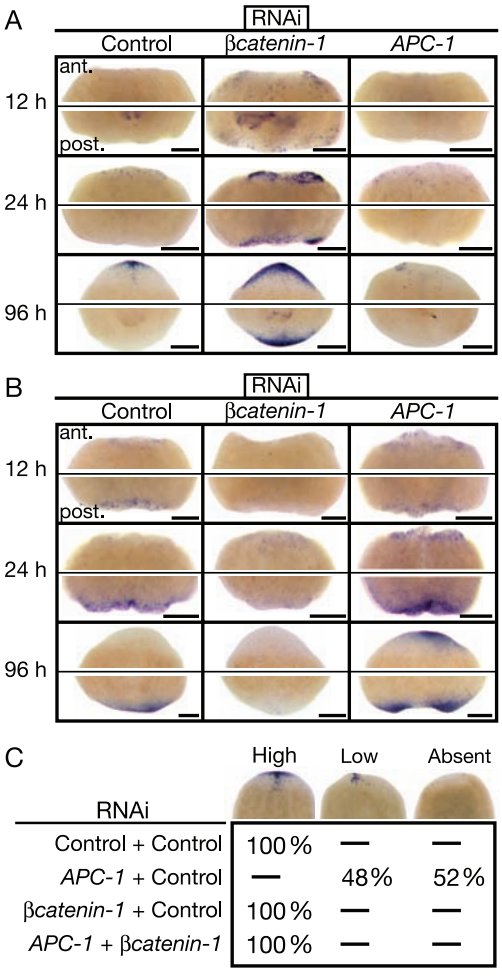

Fig. 2. *Smed-*β*catenin-1(RNAi)* and *Smed-APC-1(RNAi)* phenotypes manifest early, and the *Smed-APC-1(RNAi)* phenotype depends on *Smed-*β*catenin-1*. (**A**) Anterior (*Smed-sFRP-1*) and (**B**) posterior (*Smed-fz-4*) marker expression time course in regenerating trunk fragments. Anterior (ant.) and posterior (post.) blastemas from the same representative fragments are shown ($n \geq 15$ per condition). Scale bars, 200 μm. (**C**) Double-silencing experiments assaying *Smed-sFRP-1* expression in anterior trunk blastemas 4 days after amputation; animals were scored as high, low, or absent (see examples, top row). Proportions of scored animals are listed for each category ($n \geq 24$ per condition). Control, *unc-22(RNAi)*.

gested that regulators of β-catenin act early during regeneration. We therefore used the anterior and posterior markers to investigate the onset of blastema differentiation in control and RNAi-treated trunk fragments (Fig. 2, A and B). In control animals at 12 hours after amputation, the anterior marker was virtually undetectable, whereas the posterior marker was clearly evident in the posterior blastema; 24 hours after amputation, the two markers recapitulated the A/P specificity seen later during regeneration and in adult animals (Fig. 1, O and S; Fig. 2, A and B). However, in *Smed-*β*catenin-1(RNAi)* trunks, the anterior marker was expressed at both ends by 12 hours and maintained throughout the experiment, whereas the posterior marker remained markedly reduced (Fig. 2, A and B). The reverse was observed in *Smed-APC-1(RNAi)* trunks (Fig. 2, A and B). Consistent with the inferred time window for β-catenin signaling, *Smed-*β*catenin-1* and *Smed-APC-1* were expressed at both ends in wild-type animals by 12 hours (fig. S7). These results indicate that β-catenin and APC act very early to determine blastema identity.

We next used animals silenced for both *Smed-*β*catenin-1* and *Smed-APC-1* to test whether the *Smed-APC-1(RNAi)* phenotype results from increased β-catenin activity. Under these conditions, anterior blastemas were properly fated, indicating that the misspecification phenotype of *Smed-APC-1(RNAi)* depends on *Smed-*β*catenin-1* (Fig. 2C). Additionally, posterior blastemas adopted an anterior fate, indicating that the *Smed-*β*catenin-1(RNAi)* phenotype does not depend on APC activity. The

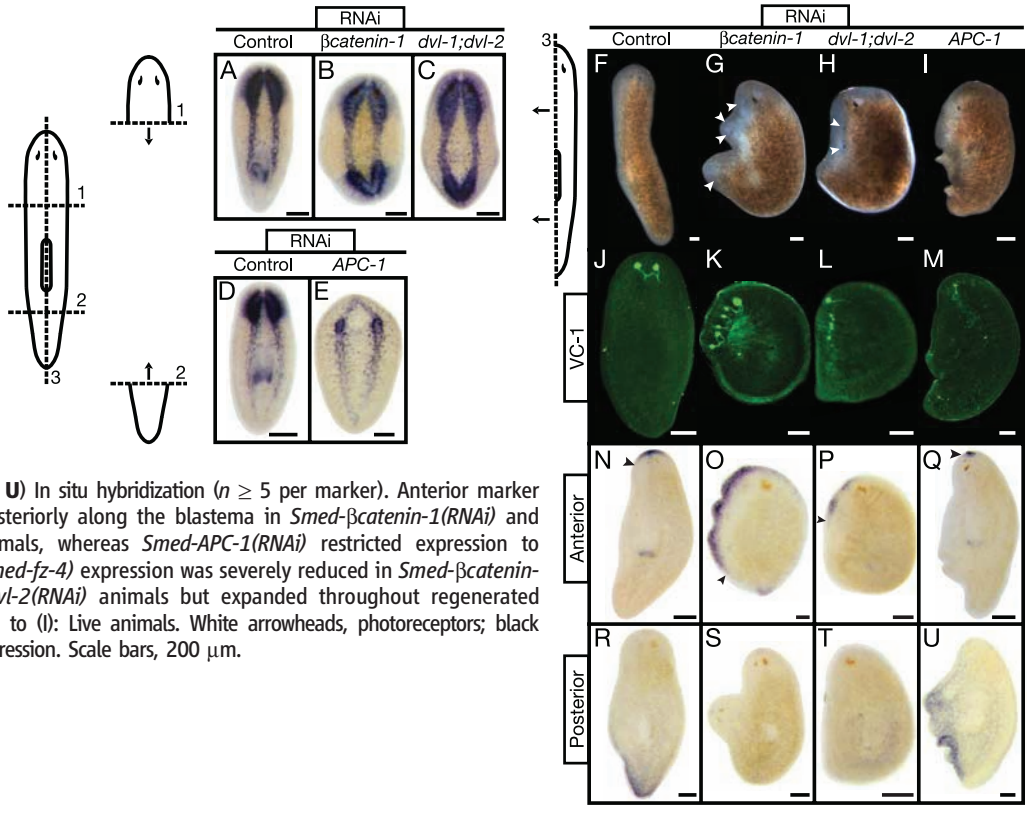

Fig. 3. *Smed-*β*catenin-1*, *Smed-dvl-1; Smed-dvl-2*, and *Smed-APC(RNAi)* phenotypes do not depend on position or orientation of amputation. Fragments 14 days after amputation are shown; control, *unc-22(RNAi)*. (**A** to **E**) PC2 in situ hybridization (CNS) ($n \geq 5$). *Smed-*β*catenin-1(RNAi)* and *Smed-dvl-1(RNAi);Smed-dvl-2(RNAi)* fragments regenerated posterior brain tissue; *Smed-APC-1(RNAi)* fragments failed to regenerate anterior brain tissue. (**F** to **M**) During lateral regeneration, *Smed-*β*catenin-1(RNAi)* and *Smed-dvl-1(RNAi);Smed-dvl-2(RNAi)* animals developed supernumerary heads and photoreceptors; *Smed-APC-1(RNAi)* prevented proper regeneration of these structures ($n \geq 15$). Photoreceptors were visualized with VC-1 antibody (*25*). (**N** to **U**) In situ hybridization ($n \geq 5$ per marker). Anterior marker (*Smed-sFRP-1*) expression expanded posteriorly along the blastema in *Smed-*β*catenin-1(RNAi)* and *Smed-dvl-1(RNAi);Smed-dvl-2(RNAi)* animals, whereas *Smed-APC-1(RNAi)* restricted expression to preexisting tissues. Posterior marker (*Smed-fz-4*) expression was severely reduced in *Smed-*β*catenin-1(RNAi)* and *Smed-dvl-1(RNAi);Smed-dvl-2(RNAi)* animals but expanded throughout regenerated tissues in *Smed-APC-1(RNAi)* animals. (F) to (I): Live animals. White arrowheads, photoreceptors; black arrowheads, extent of anterior marker expression. Scale bars, 200 μm.

combined data show that signaling through β-catenin occurs at posterior amputations and is necessary and sufficient to specify tail fate. In contrast, signaling through β-catenin is blocked or never occurs at anterior amputations, and this is necessary and sufficient to specify head fate. The premature expression of the anterior marker in *Smed-*β*catenin-1(RNAi)* worms may indicate that in wild-type planarians, β-catenin inhibition does not immediately follow amputation (Fig. 2A). We suggest that β-catenin activity acts as a molecular switch to specify head versus tail fate in planarians.

We then explored whether the β-catenin switch plays a role in blastema identity regardless of the A/P location or angle of amputation. Indeed, the head fragments of *Smed-*β*catenin-1(RNAi)* and *Smed-dvl-1(RNAi);Smed-dvl-2(RNAi)* worms regenerated a head from the posterior wound (penetrance = 79%, $n = 24$; penetrance = 82%, $n = 33$, respectively), and the tail fragments of *Smed-APC-1(RNAi)* worms regenerated a tail from the anterior wound (penetrance = 67%, $n = 27$; Fig. 3, A to E, and movie S4). After longitudinal amputation along the midline, control animals formed a blastema along the A/P axis and regenerated mediolaterally (Fig. 3, F, J, N, and R). In contrast, *Smed-*β*catenin-1(RNAi)* and *Smed-dvl-1(RNAi);Smed-dvl-2(RNAi)* worms regenerated anterior tissue and developed multiple ectopic heads along the lateral edge (Fig. 3, G, H, K, L, O, P, S, and T). The most severely affected *Smed-APC-1(RNAi)* worms regenerated posterior tissue and failed to replace the lost head structures (Fig. 3, I, M, Q, and U). Thus, the laterally regenerating tissue in RNAi-treated animals was misspecified. Our data indicate that β-catenin activity is regulated during lateral regeneration and that the β-catenin switch can dominantly misspecify regenerating tissues regardless of A/P position or amputation angle.

*Smed-*β*catenin-1(RNAi)* animals also displayed striking changes in the nonregenerating portions of regenerating fragments. *Smed-*β*catenin-1(RNAi)* tail fragments at 24 and 48 hours after amputation expressed the anterior marker in cell clusters around the circumference of the fragment (Fig. 4, A, B, D, and E). By day 14, in addition to a new head, moving head-like protrusions developed from the periphery (Fig. 4, C and F, and movie S5). Similar protrusions also developed in trunk fragments (movie S2).

Such fate changes may have been initiated by amputation. We therefore observed unamputated (intact) worms 14 days after the final RNAi feeding. Ectopic photoreceptors were visible in the tail of all ($n = 20$) *Smed-*β*catenin-1(RNAi)* animals and none of the control animals (Fig. 4, G, H, M, and N). Intact RNAi-treated animals also exhibited ectopic lateral protrusions, formed a brain in the tail region, and expressed the anterior marker posteriorly (Fig. 4, I to L and O to R, and movie S6). The molecular basis for such a change of A/P polarity in an adult organism was previously unknown.

Together, our data demonstrate the fundamental importance of β-catenin in the maintenance of polarity and cell fate during tissue regeneration and homeostasis in planarians (fig. S8). Our findings reveal a dynamic control of β-catenin in adult animals that is not readily apparent during the progression of embryogenesis: The precise quantity and location of regenerating tissue is different for each individual and for each regeneration event, newly regenerated tissues must integrate with the old, and ongoing homeostatic cell turnover may require sustained instructive cues. It is interesting that we did not observe any head or tail misspecification phenotypes for any of the upstream components of canonical Wnt signaling (Wnts, Frizzleds, or Porcupines; see table S1). Although we cannot rule out protein perdurance, incomplete gene silencing, or redundancy with known or unidentified components, the intracellular components of β-catenin signaling may be regulated by an unconventional upstream mechanism to specify polarity during regeneration and/or homeostasis. Indeed, β-catenin regulation can be Wnt-independent in vertebrate cells, and Dishevelled remains the most upstream known β-catenin regulator during early sea urchin development (*14*, *17*, *18*). With respect to putative downstream effectors, planarians can regenerate double heads after pharmacological gap junction inhibition, and β-catenin is implicated in gap junction formation and function (*19*–*21*). Finally, whether specification and maintenance of the planarian A/P axis via β-catenin is or is not independent of Hox proteins remains to be determined.

More than 100 years ago, T. H. Morgan reported that fragments with closely spaced anterior and posterior amputation planes occasionally regenerate two-headed animals (*22*, *23*). He termed these animals "Janus heads" and suggested that "something in the piece itself determines that a head shall develop at the anterior cut surface and a tail at the posterior cut surface" (*24*). Our results indicate that β-catenin activity is a key target of polarity specification in planarians, providing mechanistic insight into the old, unanswered question of how blastema fate is controlled. We propose that the evolutionarily ancient β-catenin protein, in a manner reminiscent of its role during metazoan embryogenesis (*6*, *8*), acts as a molecular switch in adult planarians and that it may play a similar role in the adult tissues of other animals.

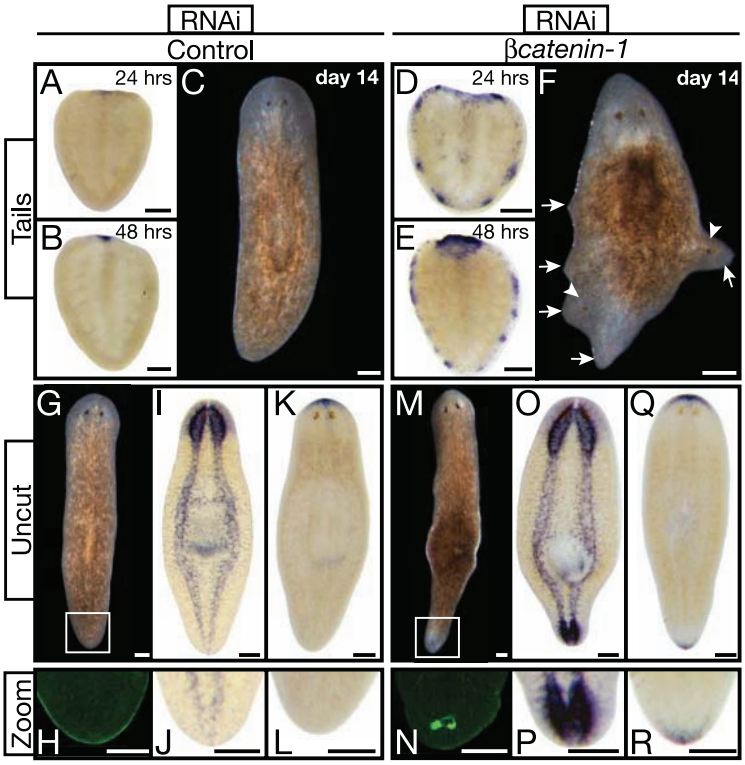

Fig. 4. *Smed-*β*catenin-1(RNAi)* transforms nonregenerating tissues. (**A** to **F**) Tail fragments. (A), (B), (D), and (E): Anterior marker (*Smed-sFRP-1*) analyses 24 and 48 hours after amputation revealed early ectopic expression in *Smed-*β*catenin-1(RNAi)* ($n \geq 5$ per condition). (C) and (F): Live tail fragments 14 days after amputation. *Smed-*β*catenin-1(RNAi)* caused lateral ectopic protrusions (arrowheads, ectopic photoreceptors; arrows, abnormal protrusions). (**G** to **R**) Transformation of tail into head tissue in uncut *Smed-*β*catenin-1(RNAi)* animals 14 days after final RNAi-feeding. (G) and (M): Live animals. (I) and (O): PC2 in situ hybridization (CNS) ($n \geq 4$). (K) and (Q): Anterior marker expression ($n \geq 4$). (H), (J), (L), (N), (P), and (R): Magnification of tail tips [boxes in (G) and (M)]. (H) and (N): VC-1 antibody staining (photoreceptors). Control, *unc-22(RNAi)*. Scale bars, 200 μm.

References and Notes

1. S. Schneider, H. Steinbeisser, R. M. Warga, P. Hausen, *Mech. Dev.* **57**, 191 (1996).
2. C. A. Larabell *et al.*, *J. Cell Biol.* **136**, 1123 (1997).

3. C. Y. Logan, J. R. Miller, M. J. Ferkowicz, D. R. McClay, *Development* **126**, 345 (1999).
4. A. H. Wikramanayake *et al.*, *Nature* **426**, 446 (2003).
5. S. Orsulic, M. Peifer, *J. Cell Biol.* **134**, 1283 (1996).
6. C. E. Rocheleau *et al.*, *Cell* **90**, 707 (1997).
7. C. E. Rocheleau *et al.*, *Cell* **97**, 717 (1999).
8. S. Q. Schneider, B. Bowerman, *Dev. Cell* **13**, 73 (2007).
9. C. Y. Logan, R. Nusse, *Annu. Rev. Cell Dev. Biol.* **20**, 781 (2004).
10. C. L. Stoick-Cooper *et al.*, *Development* **134**, 479 (2007).
11. H. Yokoyama, H. Ogino, C. L. Stoick-Cooper, R. M. Grainger, R. T. Moon, *Dev. Biol.* **306**, 170 (2007).
12. C. Kobayashi, Y. Saito, K. Ogawa, K. Agata, *Dev. Biol.* **306**, 714 (2007).
13. R. Stadeli, R. Hoffmans, K. Basler, *Curr. Biol.* **16**, R378 (2006).
14. K. Willert, K. A. Jones, *Genes Dev.* **20**, 1394 (2006).
15. M. D. Gordon, R. Nusse, *J. Biol. Chem.* **281**, 22429 (2006).
16. J. B. Wallingford, R. Habas, *Development* **132**, 4421 (2005).
17. F. H. Brembeck *et al.*, *Genes Dev.* **18**, 2225 (2004).
18. C. A. Ettensohn, *Sci. STKE* **2006**, pe48 (2006).
19. T. Nogi, M. Levin, *Dev. Biol.* **287**, 314 (2005).
20. R. M. Shaw *et al.*, *Cell* **128**, 547 (2007).
21. K. A. Guger, B. M. Gumbiner, *Dev. Biol.* **172**, 115 (1995).
22. T. H. Morgan, *Arch. Entw. Mech. Org.* **7**, 364 (1898).
23. P. W. Reddien, A. Sánchez Alvarado, *Annu. Rev. Cell Dev. Biol.* **20**, 725 (2004).
24. T. H. Morgan, *Am. Nat.* **38**, 502 (1904).
25. F. Sakai, K. Agata, H. Orii, K. Watanabe, *Zool. Sci.* **17**, 375 (2000).
26. We thank K. Agata for VC-1 antibody; B. Pearson and G. Eisenhoffer for optimization of in situ protocols; and R. Dorsky, T. Piotrowski, and all Sánchez lab members for comments. Supported by National Institute of General Medical Sciences grants F32GM082016 (K.A.G.), T32CA093247 (K.A.G.), and RO-1 GM57260 (A.S.A.) and by the European Molecular Biology Organization (J.C.R.). A.S.A. is a Howard Hughes Medical Institute Investigator. For *S. mediterranea* genes, GenBank accession numbers are EU130785, EU130786, EU130787, EU130788, EU130789, EU130790, and EU130791.

Supporting Online Material

www.sciencemag.org/cgi/content/full/1150029/DC1
Materials and Methods
Figs. S1 to S8
Tables S1
Movies S1 to S6

4 September 2007; accepted 28 November 2007
Published online 6 December 2007;
10.1126/science.1150029
Include this information when citing this paper.

*Smed-*β*catenin-1* Is Required for Anteroposterior Blastema Polarity in Planarian Regeneration

Christian P. Petersen[1] and Peter W. Reddien[1,2]*

Planarian flatworms can regenerate heads at anterior-facing wounds and tails at posterior-facing wounds throughout the body. How this regeneration polarity is specified has been a classic problem for more than a century. We identified a planarian gene, *Smed-*β*catenin-1*, that controls regeneration polarity. Posterior-facing blastemas regenerate a head instead of a tail in *Smed-*β*catenin-1(RNAi)* animals. *Smed-*β*catenin-1* is required after wounding and at any posterior-facing wound for polarity. Additionally, intact *Smed-*β*catenin-1(RNAi)* animals display anteriorization during tissue turnover. Five Wnt genes and a secreted Frizzled-related Wnt antagonist-like gene are expressed in domains along the anteroposterior axis that reset to new positions during regeneration, which suggests that Wnts control polarity through *Smed-*β*catenin-1*. Our data suggest that β-catenin specifies the posterior character of the anteroposterior axis throughout the Bilateria and specifies regeneration polarity in planarians.

The ability to regenerate is widespread and varies in degree within the animal kingdom. Planarian flatworms are dramatic examples, capable of regenerating a complete animal from nearly any fragment of the organism. Amputation induces the formation of a regeneration blastema, which differentiates to produce missing structures. Blastema formation requires adult stem cells called neoblasts (*1*). More than a century ago, Randolph (*2*) and Morgan (*3*) noted that transverse planarian pieces can regenerate a head and a tail at the anterior and posterior wound sites, respectively. Furthermore, any body region can become involved in either head or tail regeneration depending upon the identity of the missing tissue (Fig. 1A). Therefore, planarians possess a robust system throughout the anteroposterior (A-P) axis for specifying the identity of missing tissue at wounds. This system has been named "polarity." Morgan observed that very thin transverse pieces occasionally regenerate animals with two heads and hypothesized that a gradient of material establishes regeneration polarity. Although these features of planarian regeneration are frequently described in textbook examples of polarity, no previous explanation exists for the underlying genetic mechanisms that specify regeneration polarity.

The planarian *Schmidtea mediterranea* has emerged as a powerful molecular genetic system for studying regeneration because of genome sequence availability, the ability to use RNA interference (RNAi) (*4*, *5*), and the evolutionary position of the organism within an understudied protostome superphylum, the Lophotrochozoa (*6*). To study polarity in planarians, we performed an RNAi screen involving surgically removed heads and tails (Fig. 1B). We identified a single gene required for polarity and named the gene *Smed-*β*catenin-1*. The trunks of *Smed-*β*catenin-1(RNAi)* animals regenerated apparent heads at both posterior-facing and anterior-facing wounds (Fig. 1C). This dramatic phenotype is reminiscent of the polarity transformations observed in Morgan's classic surgical manipulation experiments. Double-stranded RNA (dsRNA) from *Caenorhabditis elegans unc-22*, a gene not present in planarians, served as the RNAi control (Fig. 1C). The predicted SMED-βCATENIN-1 protein is homologous to β-catenin proteins found in other animals (fig. S1A). β-catenin proteins mediate canonical Wnt signal transduction to regulate many developmental events (*7*). SMED-βCATENIN-1 possesses at least nine predicted armadillo repeats and a candidate N-terminal GSK-3β phosphorylation site (GSK-3β–mediated phosphorylation can regulate β-catenin stability) (fig. S1B) (*8*). Because armadillo repeats can be very degenerate (*9*), more armadillo repeats may exist and not be recognized in this protein. *Smed-*β*catenin-1* mRNA was broadly expressed in in situ hybridizations and reduced in *Smed-*β*catenin-1(RNAi)* animals (fig. S2).

*Smed-*β*catenin-1(RNAi)* posterior blastemas contained two apparent photoreceptors (Fig. 1C) and possessed headlike stretching behavior (n = 105/107). These posterior blastemas also contained cell types normally associated with the head, including photoreceptor neurons and cephalic ganglia (Fig. 1D). Posterior blastemas displayed local headlike polarity, with photoreceptors being more distal to the wound site than cephalic ganglia. Anterior-specific transcripts can be observed in the posterior *Smed-*β*catenin-1(RNAi)* blastemas by 72 hours after amputation (fig. S3). Additionally, *Smed-*β*catenin-1(RNAi)* posterior blastemas lacked the tail pattern of H.1.3b-zonadhesin expression (Fig. 1E). Together, these data indicate that posterior *Smed-*β*catenin-1(RNAi)* blastemas are heads.

*Smed-*β*catenin-1(RNAi)* animals regenerated posterior-facing heads at multiple A-P locations, indicating a requirement for *Smed-*β*catenin-1* throughout the A-P axis (Fig. 2A, fig. S4). We injected *Smed-*β*catenin-1* dsRNA into freshly amputated wild-type transverse fragments to inhibit *Smed-*β*catenin-1* only during regeneration. Because these animals displayed a 100% penetrant polarity reversal, *Smed-*β*catenin-1* is required during regeneration for the polarity decision (Fig. 2B). In addition, because these pieces only contained a small region of preexisting tissue, *Smed-*β*catenin-1* can be required locally.

[1]Whitehead Institute for Biomedical Research, 9 Cambridge Center, Cambridge, MA 02142, USA. [2]Department of Biology, Massachusetts Institute of Technology, Cambridge, MA 02139, USA.

*To whom correspondence should be addressed. E-mail: reddien@wi.mit.edu